Nuclear Engineering and Technology 51 (2019) 155–162

Contents lists available at ScienceDirect

Nuclear Engineering and Technology

journal homepage: www.elsevier.com/locate/net

Original Article

A leak detection and 3D source localization method on a plant piping system by using multiple cameras

Se-Oh Kim [a], Jae-Seok Park [a], Jong Won Park [b, *]

[a] SAE-AN Engineering Co., RM910, Byuksan Digital Valley II, 184, Gasan Digital 2-ro, Geumcheon-gu, Seoul, 08501, Republic of Korea
[b] Chungnam National University, 99, Daehak-ro, Yuseong-gu, Daejeon, 34134, Republic of Korea

ARTICLE INFO

Article history:
Received 30 January 2018
Received in revised form
20 September 2018
Accepted 21 September 2018
Available online 22 September 2018

Keywords:
Image processing
Camera
Steam leakage
Leakage detection
3D leakage location

ABSTRACT

To reduce the secondary damage caused by leakage accidents in plant piping systems, a constant surveillance system is necessary. To ensure leaks are promptly addressed, the surveillance system should be able to detect not only the leak itself, but also the location of the leak. Recently, research to develop new methods has been conducted using cameras to detect leakage and to estimate the location of leakage. However, existing methods solely estimate whether a leak exists or not, or only provide two-dimensional coordinates of the leakage location. In this paper, a method using multiple cameras to detect leakage and estimate the three-dimensional coordinates of the leakage location is presented. Leakage is detected by each camera using MADI(Moving Average Differential Image) and histogram analysis. The two-dimensional leakage location is estimated using the detected leakage area. The three-dimensional leakage location is subsequently estimated based on the two-dimensional leakage location. To achieve this, the coordinates (x, z) for the leakage are calculated for a horizontal section (XZ plane) in the monitoring area. Then, the y-coordinate of leakage is calculated using a vertical section from each camera. The method proposed in this paper could accurately estimate the three-dimensional location of a leak using multiple cameras.

1. Introduction

Plant piping systems are usually used to transport steam and oil at high temperature and pressure. Leakage mainly occurs in the joints or valves of pipelines due to vibrations or heat curing within the piping system. Leaks in a high-temperature, high-pressure pipe can cause enormous economic damage or even loss of lives.

In August 2004, a fatal accident occurred in Mihama nuclear power plant No. 3 due to the rupture of a steam pipe in a turbine shaft. High temperature, high pressure steam was ejected into the turbine hall, resulting in four casualties and seven injured individuals. After the accident, to ensure a prompt response in the case of leakage, several studies were conducted to detect leaks in persistent piping surveillance systems.

For leakage surveillance of piping systems, Acoustic Emission sensors are generally used. However, to detect leakage that occurs in a vast area such as a plant system, many sensors are needed, which requires a lot of manpower and high costs. Moreover, the recognition rate of a surveillance system decreases in an active piping system due to environmental noise. A study was recently conducted on leakage detection and leakage location estimation using a microphone array. However, this method was shown vulnerability due to ambient noise and reflected waves.

To resolve these problems, surveillance systems using cameras for leakage detection and leakage location estimation have been introduced [1,2,4]. This system, as presented in Fig. 1, is very simple to install and has the advantage of remote monitoring and wide-area surveillance in high temperature, highly radioactive areas.

Most existing leakage detection algorithms using cameras are focused on determining the presence of a leak. Additionally, the leakage location only displays two-dimensional coordinates. These methods cannot accurately distinguish the exact location of leakage in an area with intricate plant piping systems in three-dimensional space.

In this paper, leakage is detected using images from two cameras. In addition, the paper presents a more accurate detection approach that consists of analyzing the detected leakage area and estimating the three-dimensional coordinates. The performance of the method suggested in this paper will be examined through experiments.

* Corresponding author.
E-mail address: jwpark@cnu.ac.kr (J.W. Park).

https://doi.org/10.1016/j.net.2018.09.012

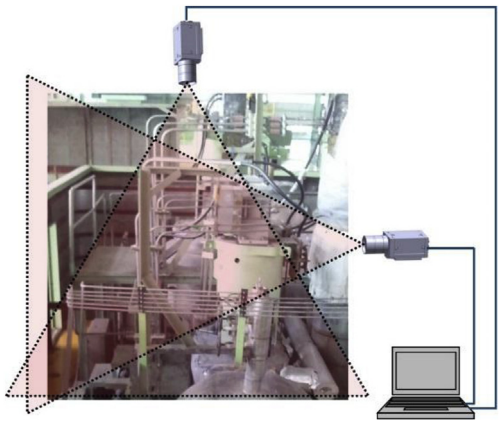

Fig. 1. Leakage detection monitoring system by using cameras.

2. Method of leak detection

To detect leakage, an existing leakage detection method was used. The method uses a MADI and histogram analysis to detect leakage [2].

2.1. Characteristic of steam leak

According to a report by Han and Park, the temperature distribution and flow velocity distribution for a leak in a high temperature, high-pressure pipe are as shown in Fig. 2 [3].

The temperature distribution of an exterior fluid varies as the pressure of the interior fluid changes. However, in a state where the inner fluid pressure remains constant, even if the inner temperature increases, the distribution of the exterior high-temperature area does not change significantly. The flow velocity distribution is affected more significantly by the pressure than the temperature of the internal fluid.

Therefore, in general, when a steam leak occurs in a high temperature, high pressure pipe, if the pressure of the pipe where leakage is occurring remains constant, the steam will leak with the same form and speed. Additionally, the area of fluid diffusion increases as the distance from the leakage location increases.

2.2. Leak detection

When a single differential image is used for leakage detection, the noise caused by external environment changes in the area may be detected as leakage. Therefore, MADI is used to detect leakage.

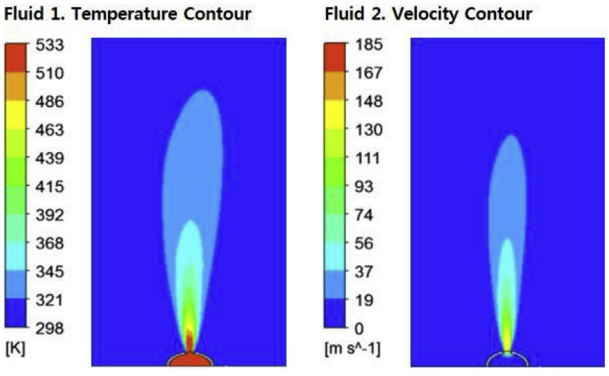

Fig. 2. Temperature distribution and flow velocity distribution of exterior fluid.

To begin, a reference image is obtained from the camera by taking an average image of a steady state without leakage. The difference between the reference image and the current image is calculated. Using the calculated differential images, the average changes is identified.

The reference image in the steady state without leakage is $R(x, y)$, the current image is $C(x, y)$, and the current time of the image is t in Eq. (1), $f_1(x, y)$, the average change of m number of images can be calculated.

$$f_1(x,y) = \frac{1}{m+1} \sum_{i=t-m}^{t} \sqrt{(C_i(x,y) - R(x,y))^2} \tag{1}$$

In the given circumstances, values with small continuance tend to have small average changes, and the values with large continuance tend to have large average changes. Therefore, the values with large continuance are the candidates for leakage.

The value $f_1(x, y)$ can contain errors caused by vibrations in the pipeline structures. Therefore, errors should be eliminated using histogram analysis.

The basic histogram analysis method is as follows. The changes caused by a leak are presented as gray-values in the histogram. However, when a leak occurs, vibrations in the pipeline structures caused by leakage pressure will not change in the histogram.

The histogram of the reference image $R(x, y)$ is R_{hist} and the histogram of the current image $C(x, y)$ is C_{hist}. The histogram difference D_{hist} can be determined as follows:

$$D_{hist} = C_{hist} - R_{hist} \tag{2}$$

Among the histogram values of D_{hist}, a value greater than 0 is a gray-value caused by leakage in the current image, and a value less than 0 is a gray-value that is lost due to leakage in the reference image. Thus, among the results of histogram analysis using the reference image and the current image, the data that satisfies Eq. (3) is $f_2(x, y)$, the candidate for leakage.

$$f_2(x,y) = \begin{cases} 1, & D_{hist}[C(x,y)] > 0 \text{ and } D_{hist}[R(x,y)] < 0 \\ 0, & \text{Others} \end{cases} \tag{3}$$

The data that satisfies f_1 and f_2 simultaneously will be considered the final leakage area.

3. Method of leak location estimation

3.1. Algorithm for leak location estimation

In this paper, leakage location is estimated in the order presented in Fig. 3. When leakage occurs, each camera analyzes images of the leak and estimates the leak location in two dimensions. Then, a method to estimate the three-dimensional leakage location based on the estimated two-dimensional leakage location is applied [4].

3.2. Two-dimensional leak location estimation

The improved leakage location estimation algorithm presented in this paper determines the contour coordinates of the leakage area using an eight-directional contour tracing algorithm [5].

The eight-directional contour tracing algorithm is implemented based on chain code. Chain code is a method that traces the boundary of a labeled area to derive the coordinates of the contour and determine the features of the contour.

After deriving the contour's coordinates, the center of gravity $C(x_c, y_c)$ in the coordinates of the contour is calculated. Then, as presented in Fig. 4, the maximum distance between the center of gravity and the coordinates of the contour is calculated.

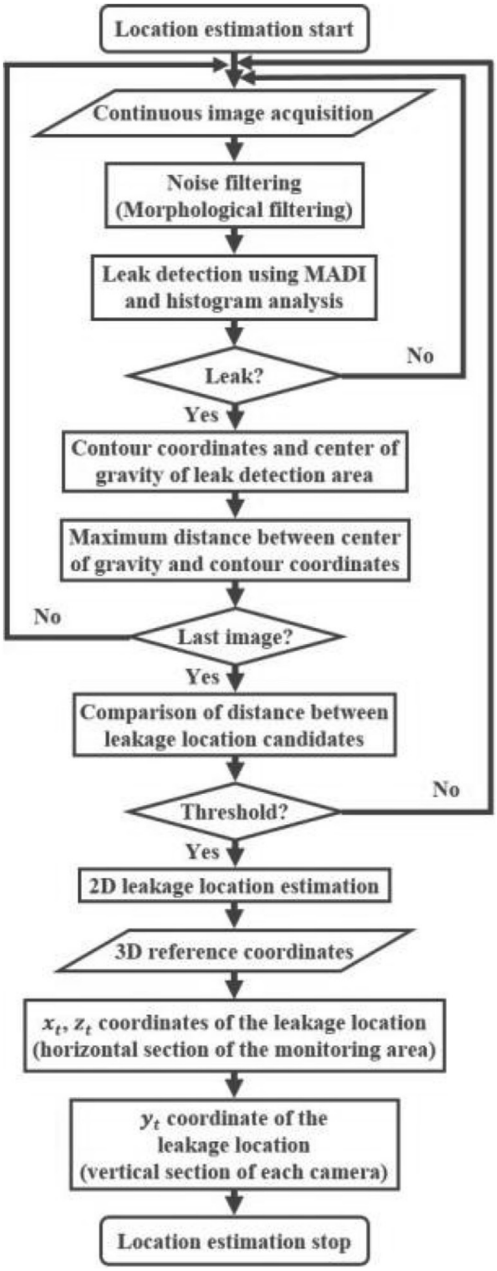

Fig. 3. Flowchart of proposed leakage location estimation.

When there are N number of coordinates in the contour, the *i-th* coordinate is referred to as $B(x_i, y_i)$ and the distance between the center of gravity and the coordinate of the contour is referred to as D_i. The maximum distance between the center of gravity and the coordinate of the contour is referred to as D_{Max}, while the function to calculate the maximum distance is referred to as *Maxdist.* The maximum distance can be determined as follows:

$$D_i = \sqrt{(x_i - x_c)^2 + (y_i - y_c)^2} \tag{4}$$

$$D_{Max} = Maxdist\ (D_i), \qquad i = 1, 2, 3, \ldots, N$$

The maximum distance previously calculated between the center of gravity and the coordinates of the contour is considered a candidate for the leakage location.

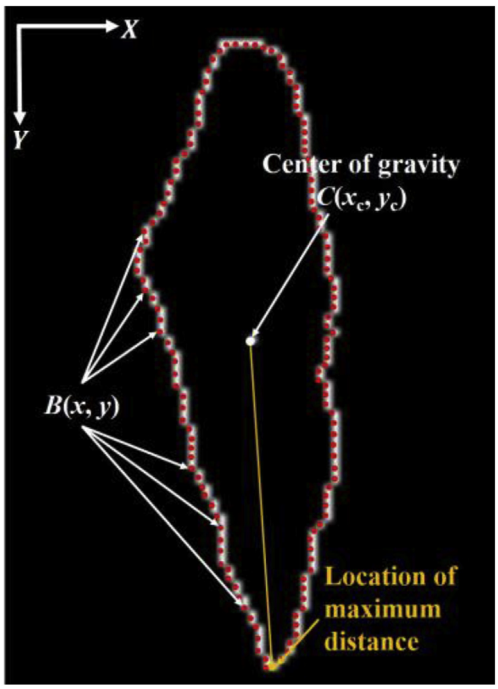

Fig. 4. Contour of the leakage area, center of gravity, location of maximum distance.

This process is applied to continuative images. Additionally, distances between the continuous extracted leakage location candidates are calculated and compared. If the distance between the leakage location candidates satisfies the threshold, the center of gravity for the candidate coordinates will be the final two-dimensional leakage location. The threshold means the boundary value of the distance between the leakage location candidates. In this paper, the leakage location estimation program was set to 5 mm. In other words, if the distance between the leakage location candidates is less than 5 mm, the center coordinate of the leakage location candidates becomes the final leakage location. This process is performed individually and simultaneously by each camera.

With the leakage detection method and the two-dimensional leakage location estimation method described previously, the two-dimensional leakage location can be estimated as presented in Fig. 5.

The determined two-dimensional leakage location is used as the base data to estimate the three-dimensional leakage location.

3.3. Three-dimensional leak location estimation

Estimation of the three-dimensional leakage location is performed using two cameras, as shown in Fig. 6. The installation venue and the direction of each camera should include a monitoring area where the possibility of leakage exists as well as the reference-coordinate for the image. The reference-coordinate is set as a point within the area where leakage is possible. In the given circumstances, the three-dimensional coordinates, $C_1(x_{c1}, y_{c1}, z_{c1})$, $C_2(x_{c2}, y_{c2}, z_{c2})$ for each camera and the reference-coordinate $R(x_r, y_r, z_r)$ have fixed values.

3.4. x, z coordinate calculation of leakage

The horizontal section of the monitoring area in Fig. 6 is the same as the *XZ* plane in Fig. 7. In this situation, $C_1(x_{c1}, y_{c1}, z_{c1})$, $C_2(x_{c2},$

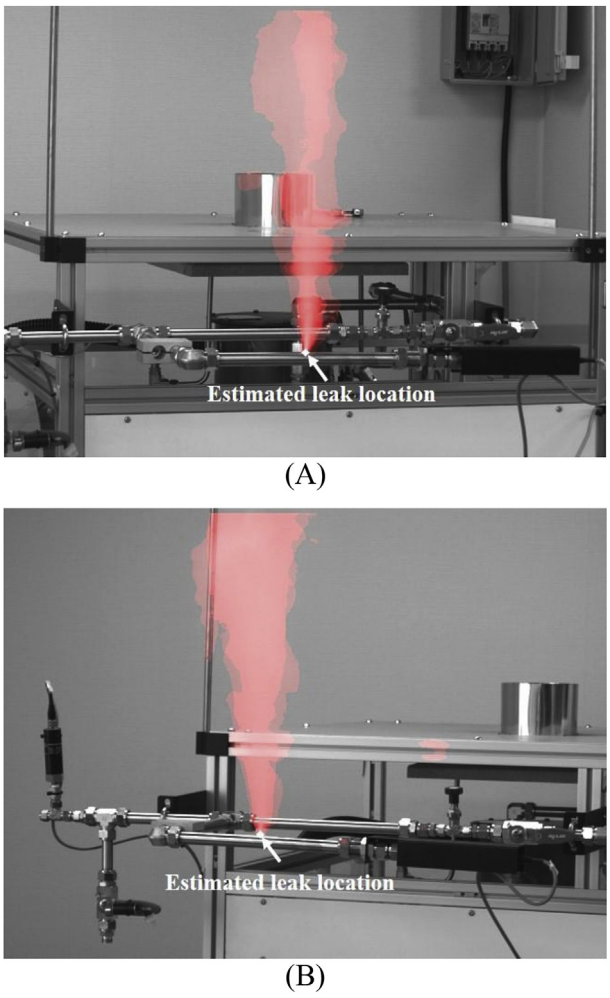

Fig. 5. Two-dimensional leakage location estimation using proposed method. (A) Estimated leakage location from Camera-1. (B) Estimated leakage location from Camera-2.

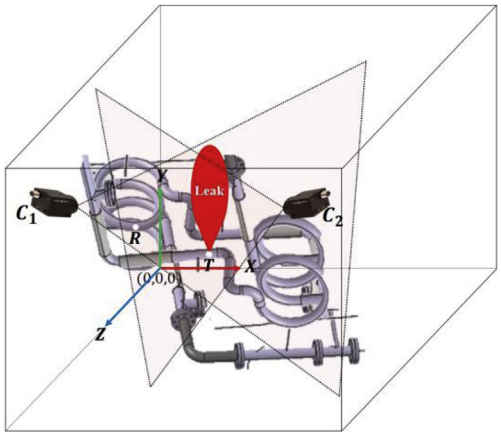

Fig. 6. Schematic diagram of three-dimensional leakage location estimation.

y_{c2}, z_{c2}), $R(x_r, y_r, z_r)$, the focal length f and the pixel size S_{size} are known.

From the XZ plane, C_1T and C_2T are calculated. C_1T refers to the straight line from the leakage-coordinate T, to the projection center of C_1. C_2T refers to the straight line from the leakage-coordinate T to

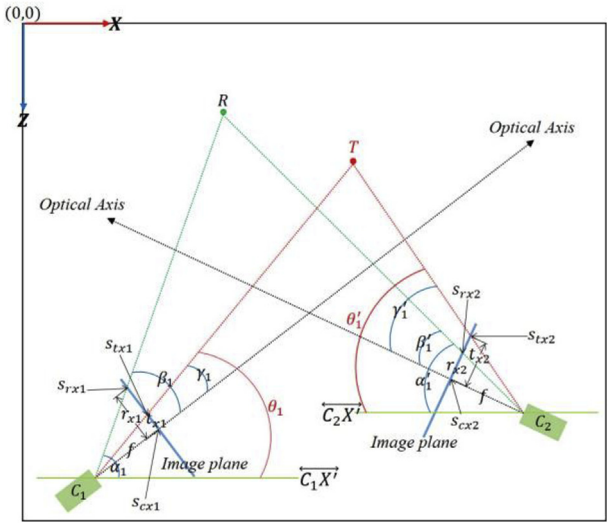

Fig. 7. XZ plane, which is the horizontal section of the monitoring area.

the projection center of C_2. The intersection of two straight lines is calculated to determine the coordinate (x_t, z_t) for T.

C_1X' is the straight line parallel to the x-axis and C_1R is the straight line from R to the projection center of C_1. The straight line C_1X' is located in the projection center of camera C_1.

In this situation, the angle formed by the straight lines C_1X' and C_1R is α_1. The angle formed by the straight line C_1R and the optic axis of C_1 is β_1. The angle formed by the straight line C_1T and the optic axis of C_1 is γ_1.

f is the focal length and S_{size} is the pixel size of the camera image sensor. s_{rx1} and s_{tx1} respectively represent the x-coordinates of the image sensor when the reference-coordinate and the two-dimensional leakage location are projected in C_1. r_{x1} and t_{x1} respectively represent the distance between s_{cx1}, the center of the image sensor of C_1, and s_{rx1} and s_{tx1}.

In the given circumstances, α_1, β_1 and γ_1 in C_1 can be determined from Eqs. (5)–(9).

$$\alpha_1 = \tan^{-1}\frac{z_r - z_{c1}}{x_r - x_{c1}} \tag{5}$$

$$\beta_1 = \tan^{-1}\frac{r_{x1}}{f} \tag{6}$$

$$\gamma_1 = \tan^{-1}\frac{t_{x1}}{f} \tag{7}$$

r_{x1} and t_{x1} can also be derived as follows:

$$r_{x1} = (s_{rx1} - s_{cx1}) \times S_{size} \tag{8}$$

$$t_{x1} = (s_{tx1} - s_{cx1}) \times S_{size} \tag{9}$$

The angle θ_1, formed at the intersection of the straight lines C_1X' and C_1T, can be calculated using Eq. (10), and the gradient of the straight line C_1T becomes $tan\theta_1$.

$$\theta_1 = \alpha_1 - \beta_1 + \gamma_1 \tag{10}$$

The gradient of the straight line C_2T, $tan\theta_1'$, can be calculated by applying the process above to C_2.

When the equation of the straight line is $y = ax + b$, the equation of the straight lines C_1T and C_2T passing through the coordinates $C_1(x_{c1}, z_{c1})$, $C_2(x_{c2}, z_{c2})$ can be defined as follows:

$$z_{c1} = \tan\theta_1 x_{c1} + b_1$$
$$z_{c2} = \tan\theta_1' x_{c2} + b_2 \quad (11)$$

The coordinate (x_t, z_t) of leakage-coordinate T, the intersection point of the straight lines C_1T and C_2T, can be calculated as follows:

$$(x_t, z_t) = \left(\frac{b_2 - b_1}{\tan\theta_1 - \tan\theta_1'}, \quad \tan\theta_1 \frac{b_2 - b_1}{\tan\theta_1 - \tan\theta_1'} + b_1 \right) \quad (12)$$

3.5. y-coordinate calculation of leakage

The vertical section of each camera is shown in Fig. 8. From the vertical section, the distance between each camera and the leakage-coordinate is calculated. C_1Z' and C_2Z', the straight lines parallel to the XZ plane, are located in the projection center of each camera. The y-coordinate of leakage-coordinate T is determined by calculating the angle formed by the straight line parallel to the plane XZ and the straight lines from T to the projection center of each camera.

The angle formed by the straight lines, C_1Z' and C_1R, is α_2, the angle formed by the optic axis of C_1 and the straight line C_1R is β_2, and the angle formed by the optic axis of C_1 and the straight line C_1T is γ_2. s_{ry1} and s_{ty1}, respectively, represent the y-coordinates of the image sensor when the reference-coordinate and two-dimensional leakage location are projected in C_1. Additionally, r_{y1} and t_{y1}, respectively, represent the distance between s_{cy1}, the center of the image sensor of C_1, and s_{ry1}, s_{ty1}.

In the given circumstances, α_2, β_2 and γ_2 for C_1 can be determined from Eqs. (13)–(19).

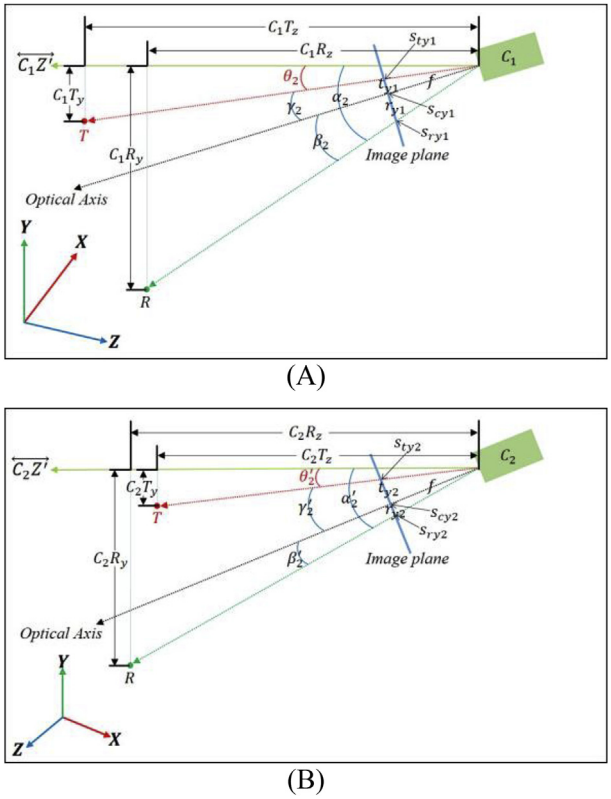

Fig. 8. Vertical section of each camera. (A) Vertical section of C_1. (B) Vertical section of C_2.

$$\alpha_2 = \tan^{-1}\frac{C_1R_y}{C_1R_z} \quad (13)$$

$$\beta_2 = \tan^{-1}\frac{r_{y1}}{f} \quad (14)$$

$$\gamma_2 = \tan^{-1}\frac{t_{y1}}{f} \quad (15)$$

C_1R_z, C_1R_y, r_{y1} and t_{y1} can also be derived as follows:

$$C_1R_z = \sqrt{(x_r - x_{c1})^2 + (z_r - z_{c1})^2} \quad (16)$$

$$C_1R_y = \sqrt{(y_r - y_{c1})^2} \quad (17)$$

$$r_{y1} = (s_{ry1} - s_{cy1}) \times S_{size} \quad (18)$$

$$t_{y1} = (s_{ty1} - s_{cy1}) \times S_{size} \quad (19)$$

The angle θ_2, formed by the straight line C_1Z' and C_1T can be calculated using Eq. (20).

$$\theta_2 = \alpha_2 - \beta_2 + \gamma_2 \quad (20)$$

Then, the angle θ_2 can be written as:

$$\tan\theta_2 = \frac{C_1T_y}{C_1T_Z} \quad (21)$$

It can be rewritten as:

$$C_1T_y = \tan\theta_2 \times C_1T_Z \quad (22)$$

C_1T_z can also be derived as follows:

$$C_1T_Z = \sqrt{(x_t - x_{c1})^2 + (z_t - z_{c1})^2} \quad (23)$$

Then, the coordinate y_{tc1} of leakage-coordinate T also can be calculated as follows:

$$y_{tc1} = y_{c1} - C_1T_y \quad (24)$$

Another y-coordinate of leakage-coordinate T, y_{tc2}, can be determined by applying the process above to C_2, and the y_t-coordinate can be calculated as follows:

$$y_t = (y_{tc1} + y_{tc2})/2 \quad (25)$$

Thus, the three-dimensional leakage location can be estimated as follows:

$$(x_t, y_t, z_t) = \left(\frac{b_2 - b_1}{\tan\theta_1 - \tan\theta_1'}, \frac{(y_{tc1} + y_{tc2})}{2}, \tan\theta_1 \frac{b_2 - b_1}{\tan\theta_1 - \tan\theta_1'} + b_1 \right) \quad (26)$$

4. Focal length of compound lens

The focal length f used in Eqs. (6), (7), (14) and (15) is the distance between the lens and the image sensor. However, the actual physical focal point changes under lens features.

In a prime lens, the distance between the lens and an object is set as S_o, the distance between the lens and an image plane as S_i, and the focal length as f. In the given circumstances, the focal length

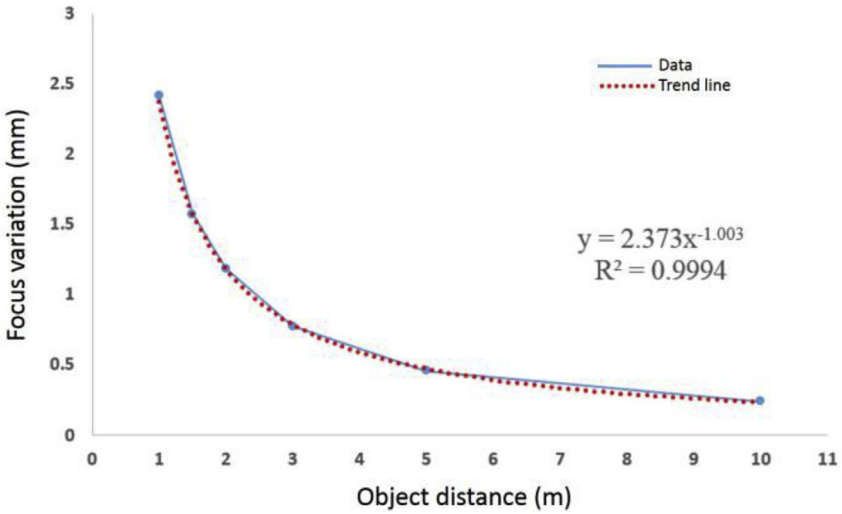

Fig. 9. Focus variation of computar M6Z1212-3S lens according to object distance.

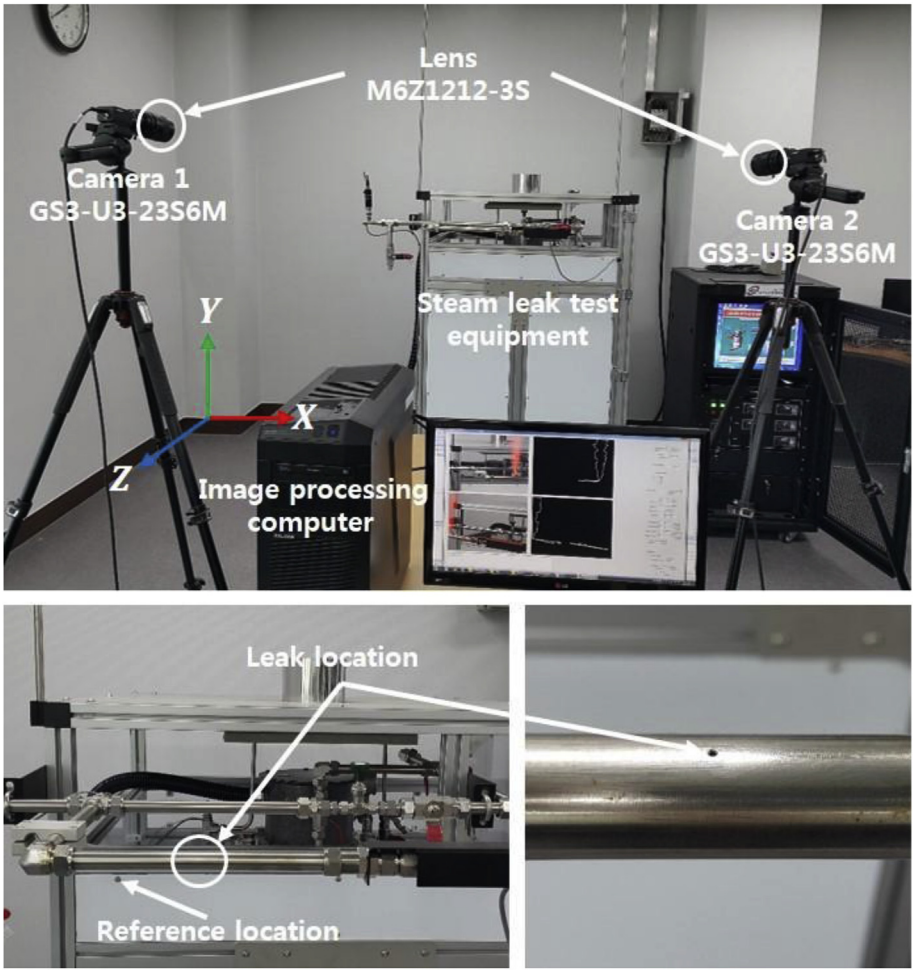

Fig. 10. Experimental setup for three-dimensional leakage location estimation.

Table 1
Results of three-dimensional leakage location estimation.

Test number	Axis	Result (mm)	Error (mm)	STD (mm)
Set 1	*x*	1958.80	3.20	1.19
	y	1448.20	3.30	1.41
	z	2008.85	0.95	1.39
Set 2	*x*	1958.65	3.45	1.60
	y	1446.70	1.70	1.68
	z	2007.50	2.10	2.31
Set 3	*x*	1962.50	1.30	1.38
	y	1447.45	3.25	1.68
	z	2006.60	3.10	2.19
Set 4	*x*	1962.10	1.70	1.26
	y	1447.00	2.00	1.33
	z	2006.55	3.35	2.70
Set 5	*x*	1962.85	2.55	1.70
	y	1447.55	2.55	2.03
	z	2007.80	3.70	0.97
Set 6	*x*	1963.10	1.70	0.47
	y	1448.20	3.20	1.39
	z	2009.30	4.30	0.47
Set 7	*x*	1962.25	1.95	0.22
	y	1448.55	3.55	0.94
	z	2009.05	5.55	0.51
Set 8	*x*	1960.85	2.25	1.68
	y	1448.75	3.75	1.74
	z	2007.05	7.05	4.19
Set 9	*x*	1963.60	2.40	1.95
	y	1446.00	1.60	0.68
	z	2002.60	7.90	3.82
Set 10	*x*	1959.45	2.65	2.39
	y	1447.75	2.75	2.09
	z	2003.75	8.35	4.05

of a prime lens can be calculated as presented in Eq. (27).

$$\frac{1}{S_o}+\frac{1}{S_i}=\frac{1}{f} \tag{27}$$

This means that as the distance between the lens and object changes, the physical focal length of the lens changes as well.

This study was conducted using a compound lens with a focal length ranging from 12.5 mm to 75 mm, which was fixed to 12.5 mm focal length during the experiments. The actual physical focal length of a compound lens also requires a change as the distance between the lens and an object changes. In this case, more complicated focal length changes are required compared to the case with prime lenses. The actual focal length of the computar M6Z1212-3S lens used in this study also depends on the distance of the object. When the object distance is 1 m, 1.5 m, 2 m, 3 m, 5 m and 10 m, the focus variations are 2.42 mm, 1.573 mm, 1.186 mm, 0.774 mm, 0.46 mm and 0.242 mm, respectively. Thus, it was necessary to accurately determine the physical focal length of the compound lens employed in this study.

Changes in the focal length of the compound lens used in this paper were calculated as presented in Fig. 9, through experiments and trend analysis.

The focus variations in the lens according to the distance from each camera are represented as Cfr_1 and Cfr_2, respectively. Through curve fitting, the focal lengths C_1af and C_2af can be calculated as follows:

$$\begin{aligned} C_1af &= \left(2.373\times(Cfr_1)^{-1.003}\right)/2 \\ C_2af &= \left(2.373\times(Cfr_2)^{-1.003}\right)/2 \end{aligned} \tag{28}$$

The actual focal lengths by distance C_1f and C_2f, can be calculated as follows:

$$\begin{aligned} C_1f &= 12.5 + C_1af \\ C_2f &= 12.5 + C_2af \end{aligned} \tag{29}$$

Thus, in Eqs. (6), (7), (14) and (15), the focal length f is presented as C_1f for C_1 and C_2f for C_2 during the study.

5. Experiments and results

To examine the suggested method, experiments were performed with the steam leak experimental equipment presented in Fig. 10.

The equipment can produce a steam leak discharge at 9 atmospheres in 250 °C through a pin hole 1 mm in diameter. The size of each pixel in the camera image sensor is 5.86 μm. A compound lens with a focal length ranging from 12.5 mm to 75 mm was used and the focal length was fixed at 12.5 mm. Thirty frames were taken per second with a resolution of 640x480 and were used to detect various leaks and perform estimation experiments.

Before performing the experiments, the three-dimensional coordinates for each camera and the reference-coordinate were determined using a laser range finder of BOSCH. The three-dimensional coordinates of actual leakage were also determined

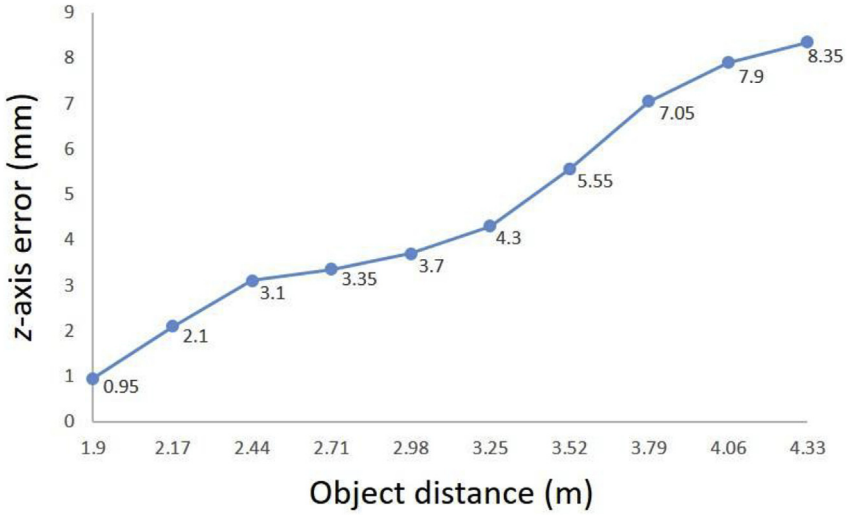

Fig. 11. *z*-axis error according to object distance.

and compared with the experimental results. The measurement accuracy of a laser range finder is ±1.5 mm.

The three-dimensional coordinates (x_t, y_t, z_t) of the pinhole where leakage occurred were 1962 mm, 1445 mm and 2008 mm. The reference-coordinates (x_r, y_r, z_r) were 1799 mm, 1290 mm and 1534 mm. The first set of positions for C_1 (x_{c1}, y_{c1}, z_{c1}) were 970 mm, 1735 mm and 3900 mm while those for C_2 (x_{c2}, y_{c2}, z_{c2}) were 3100 mm, 1735 mm and 3900 mm.

Ten sets of experiments were performed. The *X* and *Y*-coordinates of the two cameras were fixed while the *Z*-coordinate was from 1.9m to 4.33m by increasing 270 mm for each set. Table 1 shows the experimental results. The results using the proposed method were determined by averaging twenty results in each set.

EN is the number of experiments in each set. The error for the three-dimensional leakage location can be calculated as follows:

$$Error = \sqrt{\frac{1}{EN}\sum_{i=1}^{EN}(Experiment_i - Leaklocation)^2} \quad (30)$$

The error for the *x*-axis ranged from 1.3 mm to 3.45 mm while that for the *y*-axis ranged from 1.6 mm to 3.75 mm. Additionally, the *z*-axis had a error ranging from 0.95 mm to 8.35 mm, demonstrating the feasibility of estimation.

In this study, the *x*, *y*, and *z*-axes had errors of less than 10 mm. The errors included the error during leakage detection processing as well as the error from the physical resolution of the image sensors. As the distance increased in the experiments, the errors for the *z*-axis leakage location estimation increased as shown in Fig. 11. The small error in the leakage location estimation for the *x* and *y*-axes greatly affected the *z*-axis because the *z*-axis is the depth direction from the camera perspective.

When the size of the image sensor was 0.00586 mm and the focal length was 12.5 mm, the error per pixel was 1.406 mm for the estimation with a distance of 3 m.

6. Conclusions

This paper presents a new detection method using multiple cameras for surveillance in high temperature, high pressure plant piping systems, where operator access and utilization of contact sensors are limited. The suggested method estimates the leakage location in three-dimensions, analyzing the camera images when leakage occurs in a plant piping system.

For leak detection, MADI and histogram analysis were used. Additionally, to determine three-dimensional leakage location with multiple cameras, an improved two-dimensional leakage location estimation method was developed to analyze the image in the preceding stage with a single camera. From the continuant images, multiple coordinates for the maximum distances from the center of gravity to the contour of the leakage area were determined, and the leakage location with the degree of crowding for the determined coordinates was also determined.

To estimate the three-dimensional leakage location, the two-dimensional leakage locations previously calculated from each camera, the horizontal section of the leakage surveillance area (space) that includes the areas in which the cameras were installed, and the coordinate of each camera's vertical section were used.

In this paper, the potential for a more spatially accurate estimation of leakage location compared to the existing leakage location detection method was demonstrated through experiments using multiple cameras.

The experimental results showed that the error range of ten sets in the *x*-axis was ±2.32 mm, the error range of ten sets in the *y*-axis was ±2.77 mm and the error range of ten sets in the *z*-axis was ±4.64 mm. The error range of a laser range finder was ±1.5 mm. Thus, final experimental results were that ±3.82 mm in the *x*-axis, ±4.27 mm in the *y*-axis and ±6.14 mm in the *z*-axis. Additionally, the error rate was detected that 0.19% in the *x*-axis, 0.30% in the *y*-axis and 0.31% in the *z*-axis.

In conclusion, the new method proposed in this paper is considered to be viable for leakage detection in plant piping systems.

Appendix A. Supplementary data

Supplementary data to this article can be found online at https://doi.org/10.1016/j.net.2018.09.012.

References

[1] Y.C. Choi, K.S. Son, H.S. Jeon, J.H. Park, Steam leak detection by using image signal, Trans. Korean Soc. Noise Vib. Eng. 20 (9) (2010) 828–833.
[2] S.O. Kim, H.S. Jeon, K.S. Son, G.S. Chae, J.W. Park, Steam leak detection method in a pipeline using histogram analysis, J. Korean Soc. Nondestruct. Test. 35 (5) (2015) 307–313.
[3] S.W. Han, J.H. Park, D.B. Yoon, K. To, The Analysis of Heat and Flow of Nuclear Power Plant Pipes for the Simulation of Pipe Leakage, KAERI/TR-5539/2014, Fusion Technology Division, KAERI, Daejeon, 2014.
[4] S.O. Kim, H.S. Jeon, K.S. Son, J.W. Park, Location estimation method of steam leak in pipelines using leakage area analysis, J. Korean Soc. Nondestruct. Test. 36 (5) (2016) 384–390.
[5] R.C. Gonzalez, R.E. Woods, Digital Image Processing Rev. 2, Addison Wesley, Massachusetts, 1992, pp. 644–646.